Elastic buckling of single-walled carbon nanotube ropes under high pressure

C. Q. Ru*
Department of Mechanical Engineering, University of Alberta, Edmonton, Canada T6G 2G8
(Received 16 May 2000)

A modified elastic honeycomb model is presented to study elastic buckling of single-walled carbon nanotube ropes under high pressure. Simple formula is given for the critical pressure as a function of the Young's modulus and the thickness-to-radius ratio. For single-walled carbon nanotubes of diameters around 1.3 nm, the predicted critical pressure is about 1.8 GPa, which is in excellent agreement with the known data reported in the literature. This suggests that the elastic buckling would be responsible for the pressure-induced abnormalities observed for vibration modes and electric resistivity of single-walled carbon nanotube ropes.

The discovery of carbon nanotubes has stimulated extensive experimental and theoretical studies. Numerous studies showed that carbon nanotubes exhibit superior mechanical and electronic properties and hold substantial promise as new high-strength fibers and novel semiconductor materials.[1] Among various methods of research, continuum mechanics (such as elastic beam and shell) models have been widely and successfully used to study carbon nanotubes.[2] These prior studies have clearly showed that ''the laws of continuum mechanics are amazingly robust and allow one to treat even intrinsically discrete objects only a few atoms in diameter'' (Yakobson & Smalley).[1] Particularly, because experiments at the scale of nanometers are extremely difficult, and molecular dynamics simulation remains expensive for large-sized atomic system (especially for carbon nanotube ropes and multiwalled carbon nanotubes), continuum mechanics models will continue to play an essential role in the study of carbon nanotubes.

Although earlier methods for making carbon nanotubes suffered from a very much larger concentration of unwanted byproducts and a scattered distribution of diameters and geometries of carbon nanotubes, much more efficient methods with very good yields ($>75\%$) of carbon nanotubes have recently been developed,[3] that produce carbon nanotube ropes composed of aligned single-walled carbon nanotubes with narrow distribution of diameters. Thus, as a major form of carbon nanotubes, single-walled carbon nanotube ropes have widely been used in the study of carbon nanotube devices and carbon nanotube-composite materials,[4] and electronic and mechanical properties of carbon nanotube ropes have been the subject of numerous theoretical and experimental researches.[5] Here, an interesting phenomenon, which has recently been reported in the literature and motivated the present study, is the pressure-dependent abnormalities of single-walled carbon nanotube ropes.[6–9] In these works,[6–8] abrupt changes have been observed for vibration modes and electric resistivity when the applied pressure reached a critical value ranging from 1.5 to 1.9 GPa. Hence, an understanding of the intrinsic mechanism behind these pressure-induced abnormalities of carbon nanotube ropes is of great interest.

Local flattering of tube walls of carbon nanotubes due to the van der Waals forces is a well-known phenomenon.[10] Due to this effect, it has been observed that carbon nanotube ropes, especially single-walled carbon nanotubes of moderate or larger diameters, exhibit a honeycomblike geometrical structure.[4,5,10,11] In particular, when carbon nanotube ropes are exposed to a high pressure, this shape change from cylindrical to honeycomb could be enhanced considerably, and therefore carbon nanotube ropes of even smaller diameters could exhibit honeycomblike geometrical shape. Hence, the geometry of single-walled carbon nanotube ropes under high pressure can be well approximated by elastic honeycombs (hexagonal network of elastic rods or plates). In connection with this, it is noted[12–15] that elastic honeycombs under compression exhibit a remarkable structural instability when the compressive stress reaches a critical level, and this instability has been attributed to buckling of the honeycomb structure. The present study attempts to explain the aforementioned pressure-induced abnormalities of carbon nanotube ropes in terms of elastic buckling of elastic honeycomb, and to derive simple formula for the critical pressure.

To apply continuum models to carbon nanotubes, an important mechanical property of single-walled carbon nanotubes has to be clarified. Consistent with the concept established for graphite sheets, almost all previous researchers[2] have defined the equilibrium interlayer spacing between adjacent nanotubes, denoted by t (about 0.34 nm), as the representative thickness of single-walled carbon nanotubes, with the corresponding Young's modulus $E=1.1\,\mathrm{TPa}$. On the other hand, the effective bending stiffness of single-walled carbon nanotubes is 0.85 eV, while the in-plane stiffness $Et=360\,\mathrm{J/m^2}$ (see Ref. 16 and Yakobson, Brabec, and Bernhole[2]). Thus, as noted by Yakobson, Brabec, and Bernhole, the actual bending stiffness of single-walled carbon nanotubes is much (about 25 times) lower than that given by the classic formula $D=Eh^3/12$ if the thickness h is substituted by the representative thickness $t=0.34\,\mathrm{nm}$. Hence, this classic relation has to be abandoned if the representative thickness $t=0.34\,\mathrm{nm}$ is used. This inconsistency is due to single atom-layer structure of single-walled carbon nanotubes. To retain the above classic relation, as stated by Yakobson, Brabec, and Bernhole, the thickness of single-walled carbon nanotubes should be $t_0=0.066\,\mathrm{nm}$, which is about five times smaller than $t=0.34\,\mathrm{nm}$. In doing so, the corresponding Young's modulus is about $E_0=5.5\,\mathrm{TPa}$. In this paper, to be definite, the definitions of Yakobson, Brabec, and Bernhole will be followed, and then the thickness of single-walled carbon nanotubes is $t_0=0.066\,\mathrm{nm}$ and the corre-

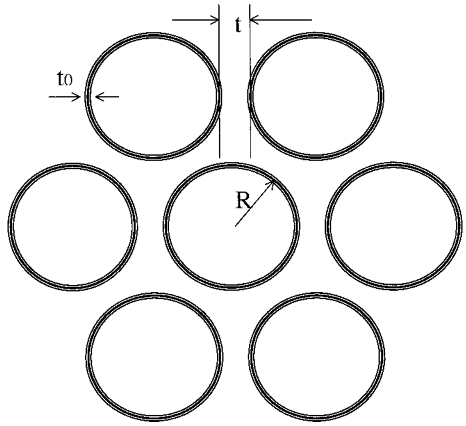

FIG. 1. Illustration of the cross section of single-walled carbon nanotube ropes.

sponding Young's modulus is $E_0 = 5.5\,\mathrm{TPa}$. Because the nearest intertube distance in carbon nanotube ropes is around $t = 0.34\,\mathrm{nm}$,[11] a consequence of the definitions of Yakobson, Brabec, and Bernhole's is that huge gaps exist between adjacent tubes, which is a few times larger than the thickness t_0, as shown in Fig. 1. As a result, the existing formulas for elastic honeycombs[12–14] cannot directly be applied to single-walled carbon nanotube ropes. Fortunately, as will be seen below, the methods of Refs. 12–14 can be modified and applied to carbon nanotube ropes to get a simple formula for the critical pressure. It should be emphasized that, as will be stated below, the predicted critical pressure stays unchanged if the representative thickness $t = 0.34\,\mathrm{nm}$, together with the corresponding Young's modulus $E = 1.1\,\mathrm{TPa}$, are adopted. In other words, the critical pressure formula obtained here does not depend whether the definition of Yakobson, Brabec, and Bernhole of the thickness of single-walled carbon nanotubes is followed or not.

In carbon nanotube ropes, the nearest intertube spacing is almost uniform and around $t = 0.34\,\mathrm{nm}$.[11] Thus, under high pressure, flattening of circular walls of carbon nanotubes leads to an approximate regular honeycomb, as shown in Fig. 2, where all edges of the regular honeycomb are approximately equal to the radius R of the single-walled carbon nanotubes, and the intertube spacing is about $t = 0.34\,\mathrm{nm}$ (the change in intertube distance due to high pressure is small and then negligible, because the hard-core component of the interatomic interaction is repulsive and strongly resists any significant reduction of the intertube spacing). A major feature which distinguishes the honeycomblike geometry of single-walled carbon nanotube ropes, shown in Fig. 2, from conventional elastic honeycombs[12–15] is that all columns of the former are hollow and composed of two thin walls separated by a distance $t = 0.34\,\mathrm{nm}$. Furthermore, the intertube friction between adjacent tubes is usually so low that any two adjacent walls could slide to each other,[17] and then bending deformation of any wall is independent of the opposing wall. Consequently, the bending stiffness of each column of the honeycomb shown in Fig. 2 is simply twice the bending stiffness of single-walled carbon nanotubes. Here, we should be reminded that the van der Waals interaction between the opposing walls does not affect the critical buckling load because the intertube spacing stays unchanged during an infinitesimal buckling of each column as a whole. This is similar to axially compressed buckling of double-walled carbon nanotubes studied in Ref. 18, where it is shown that the van der Waals forces do not affect the axial buckling strain of a double-walled carbon nanotube because buckling of the latter occurs in such a way that the interlayer spacing stays unchanged. Note that the bending stiffness of single-walled carbon nanotubes is low, as explained above. This feature of single-walled carbon nanotube ropes makes them susceptible to elastic buckling under high pressure.

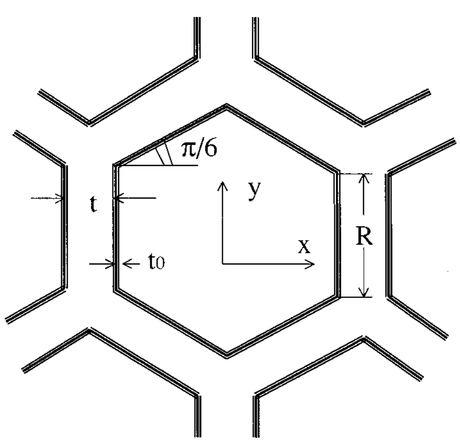

FIG. 2. Idealized cross section of a single-walled carbon nanotube in the nanotube ropes under high pressure.

According to theoretical analysis and experimental observations,[12–15] elastic honeycombs under compression buckle in two modes. The y-directional uniaxial compression and biaxial compression with the major stress in the y direction (see Fig. 2) exhibits the first mode, while biaxial compression with the major stress in the x direction exhibits the second one.[13,14] Since the essence of the methods[12–14] is clearly illustrated in the analysis of the y-directional uniaxial compression, let us first consider elastic buckling of the honeycomb formed by single-walled carbon nanotubes under uniaxial compression applied in the y direction. In this case, elastic buckling is dominated by Euler buckling of the vertical columns for which the total Euler load[19] is

$$P = \frac{-0.44\pi^2(2D)}{R^2}, D = \frac{E_0 b t_0^3}{12}, \tag{1}$$

where b is the depth of the honeycomb, 2D is the total bending stiffness of each column, and the coefficient 0.44 is a correction factor established in the literature [see e.g. (3.14) of Ref. 12, or (4.19) of Ref. 13 (1997)] which reflects the fact that the end constraint to rotation of the vertical column is between a clamped boundary (with the factor 4) and a hinged boundary (with the factor 0.25). On the other hand, the remote uniform uniaxial compressive stress σ_y and the axial force P for each column satisfy the relation

$$P = 2\sigma_y R b \cos\left[\frac{\pi}{6}\right] = \sqrt{3}\sigma_y R b, \tag{2}$$

where the interlayer spacing has been neglected as compared to the diameter. Thus, combining Eq. (1) with Eq. (2) gives the critical uniaxial compressive stress applied in the y direction as follows

$$\sigma_y \approx -0.44 E_0 \left(\frac{t_0}{R}\right)^3. \tag{3}$$

It is noted that formula (3) is different than the known formula for elastic honeycombs[12,13] by a factor of 2, because all vertical columns in the present model consist of two identical walls. In addition, the thickness $t_0 = 0.066$ nm in Eq. (3) is the thickness of a single wall carbon nanotube, while the thickness appearing in the formulas for conventional elastic honeycombs[12,13] is the total thickness of each column. Here, it should be stated that the above buckling analysis is based on elastic beam model. It is known[19] that the critical stress given by plate-buckling analysis is different from the beam model only by a factor of $1/(1-\nu^2)$, where ν is Poisson ratio. In addition, it is readily seen that the same result (3) will be obtained if the representative thickness $t = 0.34$ nm, along with the corresponding Young's modulus $E = 1.1$ TPa, are adopted. In that case, keeping in mind that the bending stiffness D in Eq. (1) is not equal to $Et^3/12$, it can be easily verified that all analysis from Eqs. (1) to (3) remain valid.

In a similar way, it is straightforward to verify that the analysis of equal-biaxial compression of conventional elastic honeycombs, given in Refs. 13 and 14 [see Sec. 4.4(b) of Ref. 13 (1997), or Appendix A of Gibson *et al.*[14]], can be extended parallel to the honeycomblike structure of single-walled carbon nanotube ropes, shown in Fig. 2. The final result is that the equal-biaxial critical stress is about 0.73 times the y-directional uniaxial critical stress. Thus, it follows from Eq. (3) that the critical pressure for elastic buckling of the honeycomb under pressure, as shown in Fig. 2, is given by

$$p_{cr} = 0.32 E_0 \frac{t_0^3}{R^3}, \quad t_0 = 0.066\,\text{nm}, \quad E_0 = 5.5\,\text{TPa}. \tag{4}$$

For example, for single-walled carbon nanotube ropes of diameters around 1.3 nm, the predicted critical pressure is about 1.8 GPa, which is in excellent agreement with the known data ranging from 1.5 to 1.9 GPa, reported in the literature.[6–8] Hence, it is believed that the elastic buckling, as described by the present honeycomb model, is responsible for the pressure-induced abnormalities of vibration modes and electrical resistivity of single-walled carbon nanotubes reported in the literature.[6–8]

As stated by some authors,[7] it would seem that the critical pressure could be estimated by studying elastic buckling of an isolated nanotube, as the center tube shown in Fig. 1. However, such a model would face several serious difficulties. First, the determination of prebuckling pressure distribution raises a troublesome task. Next, the van der Waals interaction depends on the intertube spacing between the isolated tube and the six surrounding tubes, rather than the deflection of the isolated tube alone. Hence, buckling of the isolated tube is essentially coupled with all six adjacent tubes, and this could largely complicate the analysis. The merit of the elastic honeycomb model presented here is that the coupling effect can be examined by studying column buckling of each pair of adjacent walls.

In conclusion, a simple formula is given for the critical pressure beyond which single-walled carbon nanotube ropes become elastically unstable and an abrupt change in geometrical shape will occur. Excellent agreement between the predicted critical pressure and the known data supports the validity of the model. In particular, it implies that the pressure-dependent abnormalities are not limited to vibration behavior and electric resistivity, abrupt change of other mechanical and electronic properties of single-walled carbon nanotube ropes is expected when the applied pressure reaches the same critical value. This prediction poses an interesting issue for further study.

The financial support of the Natural Science and Engineering Research Council of Canada is gratefully acknowledged.

*Email: c.ru@ualberta.ca

[1] T. W. Ebbesen, Phys. Today 26 (1994); B. I. Yakobson and R. E. Smalley, Am. Sci. **85**, 324 (1997); M. Dresselhaus, G. Dresselhaus, and R. Saito, Phys. World **1998**, 33.

[2] M. M. J. Treacy, T. W. Ebbesen, and J. M. Gibson, Nature (London) **381**, 678 (1996); E. W. Wong, P. E. Sheehan, and C. M. Lieber, Science **277**, 1971 (1997); S. Iilima, C. Brabec, A. Maiti, and J. Bernholc, J. Chem. Phys. **104**, 2089 (1996); B. I. Yakobson, C. J. Brabec, and J. Bernholc, Phys. Rev. Lett. **76**, 2511 (1996); M. R. Falvo, G. J. Clary, R. M. Taylor, V. Chi, F. P. Brooks, S. Washburn, and R. Superfine, Nature (London) **389**, 582 (1997); A. Krishnan, E. Dujardin, T. W. Ebbesen, P. N. Yianilos, and M. M. J. Treacy, Phys. Rev. B **58**, 14 013 (1998); O. Lourie, D. M. Cox, and H. D. Wagner, Phys. Rev. Lett. **81**, 1638 (1998).

[3] A. Thess, R. Lee, P. Nikolaev, H. Dai, P. Petit, J. Robert, C. Xu, Y. H. Lee, S. G. Kim, A. G. Rinzler, D. T. Colbert, G. E. Scuseria, D. Tomanek, J. E. Fisher, and R. E. Smalley, Science **273**, 483 (1996); C. Journet, W. K. Maser, P. Bernier, A. Loiseau, M. L. Chapelle, S. Lefrants, P. Deniard, R. Lee, and J. E. Fischer, Nature (London) **388**, 756 (1997).

[4] P. Poncharal, Z. L. Wang, D. Ugarte, and W. A. Heer, Science **283**, 1513 (1999); P. Kim and C. M. Lieber, *ibid.* **286**, 2148 (1999); J. P. Salvetat, J. M. Bonard, N. H. Thomson, A. J. Kulik, L. Forro, W. Benoit, and L. Zuppiroli, Appl. Phys. A: Mater. Sci. Process. **69**, 255 (1999); P. Calvert, Nature (London) **399**, 210 (1999).

[5] J. P. Lu, Phys. Rev. Lett. **79**, 1297 (1997); Y. K. Kwon, S. Saito, and D. Tomamek, Phys. Rev. B **58**, R13 314 (1998); J. P. Salvetat, G. A. D. Briggs, J. M. Bonard, R. R. Bacsa, A. J. Kulik, T. Stockli, N. A. Burnham, and L. Forro, Phys. Rev. Lett. **82**, 944 (1999); D. A. Walters, L. M. Ericson, M. J. Casavant, D. Liu, D. T. Colbert, K. A. Smith, and R. E. Smalley, Appl. Phys. Lett. **74**, 3803 (1999); S. Rols, E. Anglaret, J. L. Sauvajol, G. Coddens, and A. J. Dianoux, Appl. Phys. A: Mater. Sci. Process. **69**, 591 (1999).

[6] M. J. Peters, L. E. Mcneil, J. P. Lu, and D. Kahn, Phys. Rev. B **61**, 5939 (2000).

[7] U. D. Venkateswaran, A. M. Rao, E. Richter, M. Menon, A. Rinzler, R. E. Smalley, and P. C. Eklund, Phys. Rev. B **59**, 10 928 (1999).

[8] R. Gaal, J. P. Salvetat, and L. Forro, Phys. Rev. B **61**, 7320 (2000).

[9] D. Kahn and J. P. Lu, Phys. Rev. B **60**, 6535 (1999).

[10] R. S. Ruoff, J. Tersoff, D. C. Lorents, S. Subramoney, and B. Chan, Nature (London) **364**, 514 (1993); N. G. Chopra, L. X. Benedict, V. H. Crespi, M. L. Cohen, S. G. Louie, and A. Zettl, *ibid.* **377**, 135 (1995); J. C. Charlier, P. Lambin, T. W. Ebbesen, Phys. Rev. B **54**, R8377 (1996); T. Hertel, R. E. Walkup, and P. Avouris, *ibid.* **58**, 13 870 (1998).

[11] J. Tersoff, and R. S. Ruoff, Phys. Rev. Lett. **73**, 676 (1994); J. C. Charlier, X. Gonze, and J. P. Michenaud, Europhys. Lett. **29**, 43 (1995).

[12] L. J. Gibson, M. F. Ashby, G. S. Schajer, and C. I. Robertson, Proc. R. Soc. London, Ser. A **382**, 25 (1982).

[13] L. J. Gibson and M. F. Ashby, *Cellular Solids: Structures and Properties* (Pergamon, Oxford, 1988); 2nd ed. (Cambridge University Press, Cambridge, 1997). In particular, for conventional elastic honeycombs under the y-directional compression, it follows from (4.80) of the 1997 edition that

$$\frac{l}{2d}\left(\frac{-3\sqrt{3}l\sigma_y}{Yd}\right)^{1/2}=\frac{\pi}{6},$$

which gives the uniaxial critical stress

$$\sigma_y=-0.22Y\left(\frac{d}{l}\right)^3,$$

where Y, l, and d denote the Young's modulus, the edge length, and the thickness of the elastic honeycomb. On the other hand, for equal-biaxial compression, the two modes are coincident and then it follows from (4.80) or (4.81) that

$$\tan\left[\frac{l}{2d}\left(\frac{-12\sqrt{3}l\sigma_y}{Yd}\right)^{1/2}\right]=\sqrt{2},$$

which gives the biaxial critical stress

$$\sigma_y=-0.16Y\left(\frac{d}{l}\right)^3.$$

It is seen that the ratio of the equal-biaxial critical stress to the y-directional uniaxial critical stress is about 0.73. This conclusion remains true for the honeycomb shown in Fig. 2.

[14] L. J. Gibson, M. F. Ashby, J. Zhang, and Triantafillou, Int. J. Mech. Sci. **31**, 635 (1989); J. Zhang and M. F. Ashby, *ibid.* **34**, 491 (1992).

[15] S. D. Papak and S. Kyriakides, Int. J. Solids Struct. **35**, 239 (1998); *ibid.* **36**, 4397 (1999); N. Triantafyllidis and M. W. Schraad, J. Mech. Phys. Solids **46**, 1089 (1998); J. Chung and A. M. Waas, J. Engeg. Mater. Tech. (ASME) **121**, 494 (1999).

[16] D. H. Robertson, D. W. Brenner, and J. W. Mintmire, Phys. Rev. B **45**, 12 592 (1992).

[17] J. C. Charlier and J. P. Michenaud, Phys. Rev. Lett. **70**, 1858 (1993); R. S. Ruoff and D. C. Lorenta, Carbon **33**, 925 (1995).

[18] C. Q. Ru, J. Appl. Phys. **87**, 7227 (2000).

[19] S. P. Timoshenko and J. M. Gere, *Theory of Elastic Stability* (McGraw-Hill, New York, 1961).